PAPER Special Section on Digital Signal Processing

The Two-Dimensional Lapped Hadamard Transform*

Shogo MURAMATSU†, Akihiko YAMADA†, *and* Hitoshi KIYA†, *Members*

SUMMARY In this paper, a two-dimensional (2-D) binary-valued (BV) lapped transform (LT) is proposed. The proposed LT has basis images which take only BV elements and satisfies the axial-symmetric (AS) property. In one dimension, there is no 2-point LT with the symmetric basis vectors, and the property is achieved only with the non-overlapping basis which the Hadamard transform (HT) has. Hence, in two dimension, there is no 2×2-point separable ASLT, and only 2-D HT can be the 2×2-point separable AS orthogonal transform. By taking non-separable BV basis images, this paper shows that a 2×2-point ASLT can be obtained. Since the proposed LT is similar to HT, it is referred to as the lapped Hadamard transform (LHT). LHT of larger size is shown to be provided with a tree structure. In addition, LHT is shown to be efficiently implemented by a lattice structure.

key words: *image processing, paraunitary system, symmetric extension, lapped transform, lattice structure*

1. Introduction

Orthogonal transforms find a lot of applications in image processing, such as image analysis, recognition, and image coding [1]–[3]. They are often defined in one dimension (1D) and applied to image processing as separable multidimensional systems. We now know several useful 1D transforms for image processing, for example the Karhunen-Loeve transform, discrete cosine transform and the Hadamard transform (HT). HT is especially recognized as the simplest transform used for signal decomposition, because the basis vectors take only binary-valued (BV) elements ± 1 with a scale factor and the implementation requires no multiplication [1]. The BV elements contribute to not only the reduction of the computational complexity but also the accuracy. From the fact, for example, HT is properly applied to lossless transform coding techniques [4], [5]. In addition, the symmetric property of the basis vectors is desirable to image processing.

Recently, orthogonal transforms have been showing rapid progress as lapped transforms (LTs). In the late eighties, the special type of orthogonal transforms in which the basis vectors are overlapping was developed by Smith, Malvar etc. [6]–[8] so as to overcome some problems caused by independent block-by-block transforms, such as blocking artifacts [7], [8]. Then, the system was generalized in terms of the length of basis vectors [9]–[18], and extended to non-separable multidimensional one [19]–[21]. LTs are also known as paraunitary filter banks. Note that all LTs to be considered in this paper are orthogonal.

In 1D, it is known that there is no 2-point LT with the symmetric basis vectors, and the property is achieved only with the non-overlapping BV basis which HT has [9]. Hence, in two dimension (2D), there is no 2×2-point separable axial-symmetric (AS) LT, and only two-dimensional (2-D) HT can be the 2×2-point separable AS orthogonal transform. For 2-D LTs, the AS property is of interest since the symmetric extension method can directly be applied so as to avoid increasing the number of transform coefficients [22]–[25].

In light of the fact, we propose to construct a 2-D LT with AS basis images. We show that 2×2-point ASLTs can be obtained by introducing non-separable BV basis, and that BV-ASLT of a larger size is obtained by a tree structure. Since the proposed BV-ASLT is similar to HT, we refer to it as *the lapped Hadamard transform (LHT).* LHT can be regarded as a special type of multidimensional linear-phase paraunitary filter banks [19]–[21].

This paper is organized as follows: Section 2 reviews 2-D LTs, and Sect. 3 briefly discusses the 2-D HT. Next, Sect. 4 proposes LHT. Section 5 shows a lattice structure of LHT for its efficient implementation, followed by conclusions in Sect. 6. Throughout this paper, the following notation is used.

$\boldsymbol{z}$: a 2×1 vector which consists of variables in a 2-D z-domain, that is, $\boldsymbol{z} = (z_0 \; z_1)^T$.

$\boldsymbol{z}^{-\boldsymbol{I}}$: the vector defined by $\boldsymbol{z}^{-\boldsymbol{I}} = (z_0^{-1} \; z_1^{-1})^T$.

$\boldsymbol{z}^{\boldsymbol{n}}$: the product defined by $\boldsymbol{z}^{\boldsymbol{n}} = z_0^{n_0} z_1^{n_1}$, where $\boldsymbol{n}$ is a 2×1 integer vector, and n_k denotes the k-th element of $\boldsymbol{n}$.

$\boldsymbol{O}$: the null matrix.

$\boldsymbol{I}_M, \boldsymbol{J}_M$: the $M \times M$ identity and counter-identity matrices, respectively. When the size is obvious or not of interest, the subscript M is omitted.

$\mathcal{N}$: the set of 2×1 integer vectors.

Manuscript received December 10, 1997.
Manuscript revised March 16, 1998.

†The authors are with the Department of Electrical Engineering, Graduate School of Engineering, Tokyo Metropolitan University, Hachioji-shi, 192-0397 Japan.

*This work was presented at the 12th Digital Signal Processing Symposium.

2. Review of 2-D Lapped Transforms

In this section, we review 2-D lapped transforms (LTs), that is, 2-D maximally decimated paraunitary filter banks.

2.1 2-D Lapped Transforms

Let $\boldsymbol{M}$ be a 2×2 non-singular integer matrix and $\phi_k(\boldsymbol{n})$ for $k = 0, 1, \cdots, M-1$ be 2-D functions which satisfy the condition

$$\sum_{\boldsymbol{n}\in\mathcal{N}} \phi_k(\boldsymbol{n})\phi_{k'}^*(\boldsymbol{n}-\boldsymbol{M}\boldsymbol{m}) = \delta(k-k')\delta(\boldsymbol{m}),$$
$$k = 0, 1, \cdots, M-1,\ \boldsymbol{m}\in\mathcal{N} \quad (1)$$

for the factor-$\boldsymbol{M}$, where $M = |\det(\boldsymbol{M})|$, $\delta(\cdot)$ denotes the delta function, and $\mathcal{N}$ denotes the set of 2×1 integer vectors. Equation (1) is the extension of the *orthonormal* condition of 1-D LTs to 2-D ones and corresponds to the paraunitary condition of filter banks with the factor $\boldsymbol{M}$ [9]. The functions $\phi_k(\boldsymbol{n})$ are called *basis images.* In addition, let $\{\phi_{k,\boldsymbol{m}}\}$ be the set of the array $\phi_{k,\boldsymbol{m}}(\boldsymbol{n}) = \phi_k(\boldsymbol{n}-\boldsymbol{M}\boldsymbol{m})$, which is referred to as *basis.*

By using the basis $\{\phi_{k,\boldsymbol{m}}\}$, a 2-D LT with the factor $\boldsymbol{M}$ of an input array $x(\boldsymbol{n})$ is defined by

$$y_k(\boldsymbol{m}) = \sum_{\boldsymbol{n}\in\mathcal{N}} x(\boldsymbol{n})\phi_{k,\boldsymbol{m}}(\boldsymbol{n}), \quad (2)$$

for $k = 0, 1, \cdots, M-1$, where $y_k(\boldsymbol{m})$ denotes the k-th transform coefficient array. Then, we have the inverse LT as follows:

$$x(\boldsymbol{n}) = \sum_{k=0}^{M-1}\sum_{\boldsymbol{m}\in\mathcal{N}} y_k(\boldsymbol{m})\phi_{k,\boldsymbol{m}}^*(\boldsymbol{n}). \quad (3)$$

If the elements in the basis images $\phi_k(\boldsymbol{n})$ are real, Eq. (1) is reduced to $\sum_{\boldsymbol{n}\in\mathcal{N}} \phi_k(\boldsymbol{n})\phi_{k'}(\boldsymbol{n}-\boldsymbol{M}\boldsymbol{m}) = \delta(k-k')\delta(\boldsymbol{m})$. In this paper, for the sake of convenience, the transform as in Eq. (2) is referred to as a matrix-$\boldsymbol{M}$ transform.

In general, the support region of basis images overlaps with that of blocks adjacent to the target one as shown in Fig. 1. Note that the 2-D HT consists of non-overlapping basis images, and that orthogonal transforms are not LTs with such basis images.

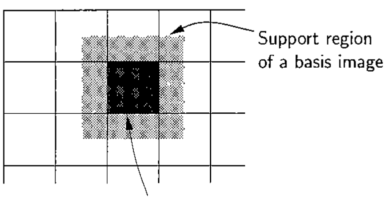

Fig. 1 Support region of a basis image in 2-D LT.

2.2 Relation to 2-D Filter Banks

Next, let us show the relation of LTs to filter banks. Figure 2 (a) shows a parallel structure of 2-D maximally decimated filter banks with a factor $\boldsymbol{M}$, where the number of decomposition is $M = |\det(\boldsymbol{M})|$. The whole system consists of an analysis and a synthesis bank. The analysis bank decomposes an input array $X(\boldsymbol{z})$ into M subband signals $Y_k(\boldsymbol{z})$, and the counterpart synthesis bank reconstructs the input array from the subband signals $Y_k(\boldsymbol{z})$. In Fig. 2 (a), $\downarrow\boldsymbol{M}$ and $\uparrow\boldsymbol{M}$ denote the down- and up-samplers with the factor $\boldsymbol{M}$, respectively. $H_k(\boldsymbol{z})$ and $F_k(\boldsymbol{z})$ are analysis and synthesis filters, respectively.

Decomposed each filter into the polyphase filters, the parallel structure can be equivalently represented as the structure shown in Fig. 2 (b), where $\boldsymbol{E}(\boldsymbol{z})$ is the type-I polyphase matrix of analysis bank and $\boldsymbol{R}(\boldsymbol{z})$ is the type-II polyphase matrix of synthesis bank [9]. If the polyphase matrix $\boldsymbol{E}(\boldsymbol{z})$ satisfies Eq. (4), then it is said to be *paraunitary* [9].

$$\tilde{\boldsymbol{E}}(\boldsymbol{z})\boldsymbol{E}(\boldsymbol{z}) = \boldsymbol{E}(\boldsymbol{z})\tilde{\boldsymbol{E}}(\boldsymbol{z}) = \boldsymbol{I}_M, \quad (4)$$

where $\tilde{\boldsymbol{E}}(\boldsymbol{z}) = \boldsymbol{E}_*^T(\boldsymbol{z}^{-\boldsymbol{I}})$, that is, the paraconjugate of $\boldsymbol{E}(\boldsymbol{z})$ [9]. This condition guarantees that $\hat{X}(\boldsymbol{z}) = X(\boldsymbol{z})$ by choosing $f_k(\boldsymbol{n}) = h_k^*(-\boldsymbol{n})$, where $h_k(\boldsymbol{n})$ and $f_k(\boldsymbol{n})$ denote impulse responses of the analysis and synthesis filters, respectively. If the filter coefficients are real, it is reduced to $f_k(\boldsymbol{n}) = h_k(-\boldsymbol{n})$.

It can be verified that analysis and synthesis process in a paraunitary system is identical to the LTs in Eqs. (2) and (3), respectively, under the condition that

$$h_k(\boldsymbol{n}) = \phi_k(-\boldsymbol{n}), \quad (5)$$

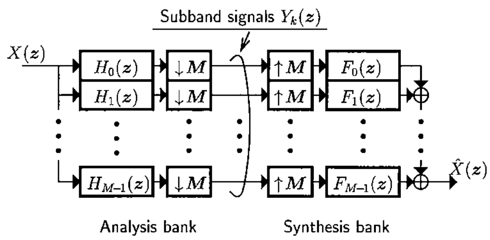

(a) Parallel structure

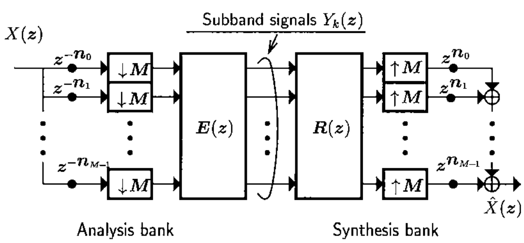

(b) Polyphase structure

Fig. 2 Structures of 2-D filter banks.

$$f_k(\boldsymbol{n}) = \phi_k^*(\boldsymbol{n}). \tag{6}$$

2.3 Axial-Symmetric Property

For 2-D LTs, the AS property is of interest because it is sufficient to the point-wise symmetry of basis, that is, the linear-phase property of filter banks, and the symmetric extension method can directly be used [23].

The AS property of a basis image $\phi_k(\boldsymbol{n})$ is expressed as follows:

$$\phi_k(\boldsymbol{n}) = \phi_k\begin{pmatrix} n_0 \\ n_1 \end{pmatrix} = \pm\phi_k\begin{pmatrix} 2c_0 - n_0 \\ n_1 \end{pmatrix}, \tag{7}$$

$$\phi_k(\boldsymbol{n}) = \phi_k\begin{pmatrix} n_0 \\ n_1 \end{pmatrix} = \pm\phi_k\begin{pmatrix} n_0 \\ 2c_1 - n_1 \end{pmatrix}, \tag{8}$$

where c_d is an integer multiple of $1/2$ and denotes the center of symmetry in the d-th dimension. Furthermore, the vector $\boldsymbol{c} = (c_0\ c_1)^T$ denotes the center of the point-wise symmetry, where $\boldsymbol{c} \in \frac{1}{2}\mathcal{N}$.

3. Review of 2-D Hadamard Transform

As a preliminary, we here review the 2-D HT and summarize its properties. Firstly, let us define a diagonal matrix $\boldsymbol{M}_p$ by

$$\boldsymbol{M}_p = \begin{pmatrix} 2^p & 0 \\ 0 & 2^p \end{pmatrix}. \tag{9}$$

In the following, the matrix-$\boldsymbol{M}_p$ transform means $2^p \times 2^p$-point one.

3.1 The 2 × 2 Hadamard Transform

Let $\phi_{\mathrm{H}k}^{(p)}(\boldsymbol{n})$ be the k-th basis image of the matrix-$\boldsymbol{M}_p$ HT. For the factor $\boldsymbol{M} = \boldsymbol{M}_1$, the basis images of HT are defined by

$$\boldsymbol{\Phi}_{\mathrm{H}0}^{(1)} = \frac{1}{2}\begin{pmatrix} 1 & 1 \\ 1 & 1 \end{pmatrix}, \tag{10}$$

$$\boldsymbol{\Phi}_{\mathrm{H}1}^{(1)} = \frac{1}{2}\begin{pmatrix} 1 & -1 \\ 1 & -1 \end{pmatrix}, \tag{11}$$

$$\boldsymbol{\Phi}_{\mathrm{H}2}^{(1)} = \frac{1}{2}\begin{pmatrix} 1 & 1 \\ -1 & -1 \end{pmatrix}, \tag{12}$$

$$\boldsymbol{\Phi}_{\mathrm{H}3}^{(1)} = \frac{1}{2}\begin{pmatrix} 1 & -1 \\ -1 & 1 \end{pmatrix}, \tag{13}$$

where $\boldsymbol{\Phi}_{\mathrm{H}k}^{(1)}$ is the matrix representation of the basis image $\phi_{\mathrm{H}k}^{(1)}(\boldsymbol{n})$, that is, $[\boldsymbol{\Phi}_{\mathrm{H}k}^{(1)}]_{n_0,n_1} = \phi_{\mathrm{H}k}^{(1)}(\boldsymbol{n}) = \phi_{\mathrm{H}k}^{(1)}\begin{pmatrix} n_0 \\ n_1 \end{pmatrix}$ for $n_0, n_1 = 0, 1$, where we assume that $\phi_{\mathrm{H}k}^{(1)}\begin{pmatrix} n_0 \\ n_1 \end{pmatrix} = 0$ for $n_0 \neq 0, 1$ or $n_1 \neq 0, 1$.

3.2 Tree Structure of the $2^p \times 2^p$ HT

The basis images of the matrix-$\boldsymbol{M}_p$ HT can be simply obtained as

$$\boldsymbol{\Phi}_{\mathrm{H}k}^{(p)} = \boldsymbol{\Phi}_{\mathrm{H}((k))_4}^{(1)} \otimes \boldsymbol{\Phi}_{\mathrm{H}\lfloor \frac{k}{4} \rfloor}^{(p-1)}, \tag{14}$$

for $k = 0, 1, \cdots, M-1$, where $((x))_N$ and $\lfloor x \rfloor$ denote the integer of x modulo N and the integer value of x, respectively, and $M = 2^{p+1}$. The operator '$\otimes$' denotes the Kronecker product.

Equation (14) implies that the matrix-$\boldsymbol{M}_p$ HT can be implemented with the p-level tree structure of the matrix-$\boldsymbol{M}_1$ HT as shown in Fig. 3, where the box including $\{\phi_{\mathrm{H}k,\boldsymbol{m}}^{(1)}\}$ denotes the matrix-$\boldsymbol{M}_1$ HT. On the other hand, the inverse transform is implemented by reversing the direction of each arrow in Fig. 3. For the sake of simplification, we take no attention to the ordering of the basis images, such as the sequency [1].

The basis images of HT does not overlap with themselves by shifting with the factor $\boldsymbol{M}_p$. Hence, we have

$$\sum_{\boldsymbol{m}\in\mathcal{N}} \phi_{\mathrm{H}k}^{(p)}(\boldsymbol{n} - \boldsymbol{M}_p\boldsymbol{m}) = \phi_{\mathrm{H}k}^{(p)}(\boldsymbol{n}),\ \boldsymbol{n} \in \mathcal{N}(\boldsymbol{M}_p), \tag{15}$$

where $\mathcal{N}(\boldsymbol{M})$ denotes the set of the integer vectors in the fundamental parallelepiped generated by $\boldsymbol{M}$ [9]. In this case, the condition as in Eq. (1) is reduced to

$$\langle \boldsymbol{\Phi}_{\mathrm{H}k}^{(p)}, \boldsymbol{\Phi}_{\mathrm{H}k'}^{(p)} \rangle = \sum_{\boldsymbol{n}\in\mathcal{N}} \phi_{\mathrm{H}k}^{(p)}(\boldsymbol{n})\phi_{\mathrm{H}k'}^{(p)*}(\boldsymbol{n}) = \delta(k - k'), \tag{16}$$

where the notation $\langle \boldsymbol{A}, \boldsymbol{B} \rangle$ expresses the sum of the element-by-element products of two matrices $\boldsymbol{A}$ and $\boldsymbol{B}$. It can be easily verified that the basis of 2-D HT satisfies the orthonormal property in Eq. (16) and are AS.

In the following, we summarize the properties of the 2-D HT.

- The basis $\{\phi_{\mathrm{H}k,\boldsymbol{m}}^{(p)}\}$ is orthonormal. In addition, the basis images $\phi_{\mathrm{H}k}^{(p)}(\boldsymbol{n})$ are AS, take only BV elements, and have no DC gain for $k \neq 0$, that is, there is no DC leakage [11].

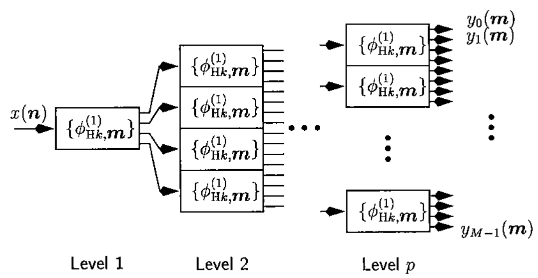

Fig. 3 The tree structure of the $2^p \times 2^p$ 2-D HT.

- The basis images $\phi_{\mathrm{H}k}^{(p)}(\boldsymbol{n})$ are *separable* and *non-overlapping*.

4. Lapped Hadamard Transform

In this section, we propose a 2-D binary-valued axial-symmetric lapped transform (BV-ASLT), which is similar to the 2-D HT. The main difference of our proposed BV-ASLT from HT is that it consists of a non-separable overlapping basis. In this paper, we refer to the proposed BV-ASLT as the *lapped Hadamard transform (LHT)*.

4.1 The 2×2 Lapped Hadamard Transform

Let $\boldsymbol{\Theta}$ be a real matrix of size 2×2 which satisfies the following condition:

$$\langle \boldsymbol{\Theta}, \boldsymbol{J}^i\boldsymbol{\Theta}\boldsymbol{J}^j\rangle = \sum_{\boldsymbol{n}\in\mathcal{N}} s_{00}(\boldsymbol{n})s_{ij}(\boldsymbol{n}) = \frac{1}{4}\delta(i)\delta(j), \tag{17}$$

for $i, j = 0, 1$, where $\boldsymbol{J}^0 = \boldsymbol{I}$, $\boldsymbol{J}^1 = \boldsymbol{J}$ and $s_{ij}(\boldsymbol{n}) = s_{ij}\begin{pmatrix} n_0 \\ n_1 \end{pmatrix} = [\boldsymbol{J}^i\boldsymbol{\Theta}\boldsymbol{J}^j]_{n_0,n_1}$ for $n_0, n_1 = 0, 1$, where we assume that $s_{ij}(\boldsymbol{n}) = s_{ij}\begin{pmatrix} n_0 \\ n_1 \end{pmatrix} = 0$ for $n_0 \neq 0, 1$ or $n_1 \neq 0, 1$.

By using the matrix $\boldsymbol{\Theta}$, we can obtain the following AS basis images $\phi_{\mathrm{L}k}^{(1)}(\boldsymbol{n})$ for the factor $\boldsymbol{M}_1$:

$$\boldsymbol{\Phi}_{\mathrm{L}0}^{(1)} = \begin{pmatrix} \boldsymbol{\Theta} & \boldsymbol{\Theta}\boldsymbol{J} \\ \boldsymbol{J}\boldsymbol{\Theta} & \boldsymbol{J}\boldsymbol{\Theta}\boldsymbol{J} \end{pmatrix}, \tag{18}$$

$$\boldsymbol{\Phi}_{\mathrm{L}1}^{(1)} = \begin{pmatrix} \boldsymbol{\Theta} & -\boldsymbol{\Theta}\boldsymbol{J} \\ \boldsymbol{J}\boldsymbol{\Theta} & -\boldsymbol{J}\boldsymbol{\Theta}\boldsymbol{J} \end{pmatrix}, \tag{19}$$

$$\boldsymbol{\Phi}_{\mathrm{L}2}^{(1)} = \begin{pmatrix} \boldsymbol{\Theta} & \boldsymbol{\Theta}\boldsymbol{J} \\ -\boldsymbol{J}\boldsymbol{\Theta} & -\boldsymbol{J}\boldsymbol{\Theta}\boldsymbol{J} \end{pmatrix}, \tag{20}$$

$$\boldsymbol{\Phi}_{\mathrm{L}3}^{(1)} = \begin{pmatrix} \boldsymbol{\Theta} & -\boldsymbol{\Theta}\boldsymbol{J} \\ -\boldsymbol{J}\boldsymbol{\Theta} & \boldsymbol{J}\boldsymbol{\Theta}\boldsymbol{J} \end{pmatrix}, \tag{21}$$

where $[\boldsymbol{\Phi}_{\mathrm{L}k}^{(1)}]_{n_0,n_1} = \phi_{\mathrm{L}k}^{(1)}(\boldsymbol{n}) = \phi_{\mathrm{L}k}^{(1)}\begin{pmatrix} n_0 \\ n_1 \end{pmatrix}$ for $n_0, n_1 = 0, 1, 2, 3$, where we assume that $\phi_{\mathrm{L}k}^{(1)}(\boldsymbol{n}) = \phi_{\mathrm{L}k}^{(1)}\begin{pmatrix} n_0 \\ n_1 \end{pmatrix} = 0$ for $n_0 \neq 0, 1, 2, 3$ or $n_1 \neq 0, 1, 2, 3$. In the following, we verify the fact that these basis images construct orthonormal basis.

From Eq. (17), since

$$\langle \boldsymbol{\Phi}_{\mathrm{L}k}^{(1)}, \boldsymbol{\Phi}_{\mathrm{L}k'}^{(1)}\rangle = \sum_{\boldsymbol{n}\in\mathcal{N}} \phi_{\mathrm{L}k}^{(1)}(\boldsymbol{n})\phi_{\mathrm{L}k'}^{(1)}(\boldsymbol{n}) = \delta(k - k'), \tag{22}$$

the orthonormality between the basis images is guaranteed. In addition, since

$$\langle \boldsymbol{\Theta}, \boldsymbol{\Theta}\boldsymbol{J}\rangle \pm \langle \boldsymbol{J}\boldsymbol{\Theta}, \boldsymbol{J}\boldsymbol{\Theta}\boldsymbol{J}\rangle = 0, \tag{23}$$

$$\langle \boldsymbol{\Theta}, \boldsymbol{J}\boldsymbol{\Theta}\rangle \pm \langle \boldsymbol{\Theta}\boldsymbol{J}, \boldsymbol{J}\boldsymbol{\Theta}\boldsymbol{J}\rangle = 0, \tag{24}$$

$$\langle \boldsymbol{\Theta}, \boldsymbol{J}\boldsymbol{\Theta}\boldsymbol{J}\rangle = \langle \boldsymbol{\Theta}\boldsymbol{J}, \boldsymbol{J}\boldsymbol{\Theta}\rangle = 0, \tag{25}$$

the orthogonality with respect to the shift by the matrix $\boldsymbol{M}_1$ is guaranteed as

$$\langle \boldsymbol{S}_{0,m_1}\boldsymbol{\Phi}_{\mathrm{L}k}^{(1)}\boldsymbol{S}_{0,m_0}^T, \boldsymbol{S}_{1,m_1}\boldsymbol{\Phi}_{\mathrm{L}k'}^{(1)}\boldsymbol{S}_{1,m_0}^T\rangle = \sum_{\boldsymbol{n}\in\mathcal{N}} \phi_{\mathrm{L}k}^{(1)}(\boldsymbol{n})\phi_{\mathrm{L}k'}^{(1)}(\boldsymbol{n} - \boldsymbol{M}_1\boldsymbol{m}) = \delta(\boldsymbol{m}),$$
$$\text{for } \boldsymbol{m} = \begin{pmatrix} m_0 \\ m_1 \end{pmatrix} \in \left\{ \begin{pmatrix} 0 \\ 0 \end{pmatrix}, \begin{pmatrix} 1 \\ 0 \end{pmatrix}, \begin{pmatrix} 0 \\ 1 \end{pmatrix}, \begin{pmatrix} 1 \\ 1 \end{pmatrix} \right\} \tag{26}$$

where $\boldsymbol{S}_{01} = (\boldsymbol{I}_2\ \boldsymbol{O})$, $\boldsymbol{S}_{11} = (\boldsymbol{O}\ \boldsymbol{I}_2)$ and $\boldsymbol{S}_{i0} = \boldsymbol{I}_4$ for $i = 0, 1$. Hence, the basis $\{\phi_{\mathrm{L}k,\boldsymbol{m}}^{(1)}\}$ satisfies the orthonormality as in Eq. (1).

Here, we have one choice of the matrix $\boldsymbol{\Theta}$ such as

$$\boldsymbol{\Theta} = \frac{1}{4}\begin{pmatrix} -1 & 1 \\ 1 & 1 \end{pmatrix}. \tag{27}$$

From the definition, the above choice generates the fol-

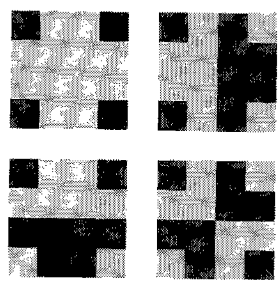

(a) Basis images.

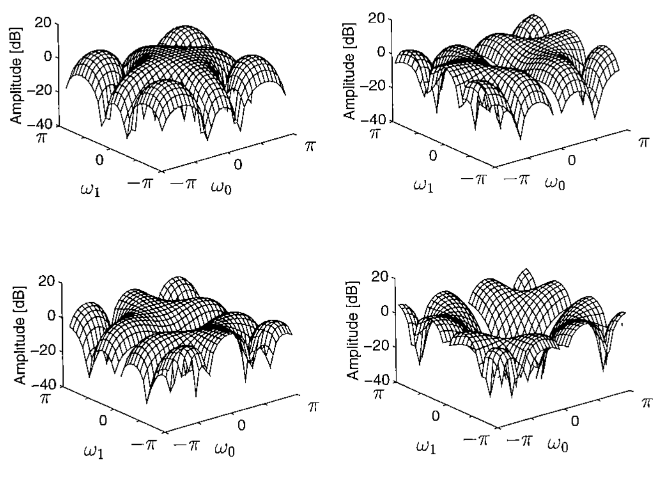

(b) Amplitude responses.

Fig. 4 The type-I lapped Hadamard transform.

lowing LT basis images:

$$\boldsymbol{\Phi}_{\mathrm{L0}}^{(1)} = \frac{1}{4}\begin{pmatrix} -1 & 1 & 1 & -1 \\ 1 & 1 & 1 & 1 \\ 1 & 1 & 1 & 1 \\ -1 & 1 & 1 & -1 \end{pmatrix}, \tag{28}$$

$$\boldsymbol{\Phi}_{\mathrm{L1}}^{(1)} = \frac{1}{4}\begin{pmatrix} -1 & 1 & -1 & 1 \\ 1 & 1 & -1 & -1 \\ 1 & 1 & -1 & -1 \\ -1 & 1 & -1 & 1 \end{pmatrix}, \tag{29}$$

$$\boldsymbol{\Phi}_{\mathrm{L2}}^{(1)} = \frac{1}{4}\begin{pmatrix} -1 & 1 & 1 & -1 \\ 1 & 1 & 1 & 1 \\ -1 & -1 & -1 & -1 \\ 1 & -1 & -1 & 1 \end{pmatrix}, \tag{30}$$

$$\boldsymbol{\Phi}_{\mathrm{L3}}^{(1)} = \frac{1}{4}\begin{pmatrix} -1 & 1 & -1 & 1 \\ 1 & 1 & -1 & -1 \\ -1 & -1 & 1 & 1 \\ 1 & -1 & 1 & -1 \end{pmatrix}. \tag{31}$$

Note that the transform with the above basis images consist of only BV elements ± 1 with the scale factor $1/4$, which implies that the transform requires no multiplication. In Fig. 4, we give the basis images, and also the amplitude responses by regarding them as analysis filters in filter banks.

The matrix $\boldsymbol{\Theta}$ is not unique, and therefore, we refer to the transform with this basis as the type-I LHT in this paper. In the following, we give another choice of the matrix $\boldsymbol{\Theta}$.

$$\boldsymbol{\Theta} = \frac{1}{4}\begin{pmatrix} -1 & -1 \\ -1 & 1 \end{pmatrix}. \tag{32}$$

Figure 5 shows the corresponding basis images and the amplitude responses. In this paper, we refer the transform as the type-II LHT.

Assume that the matrix $\boldsymbol{\Theta}$ consists of non-zero elements. In fact, on this assumption, it can be shown that $\boldsymbol{\Theta}$ must be BV with the absolute value $1/4$. In addition, if and only if the number of negative elements in $\boldsymbol{\Theta}$ is odd, that is one or three, Eq. (17) is satisfied. This implies that there are 8 choices of the matrix $\boldsymbol{\Theta}$ (see Appendix A). Note that, if the elements are not restricted to be non-zero, we have more choices, such as the HT, which are trivial.

4.2 Tree Structure of the $2^p \times 2^p$ LHT

Let us define the basis images of the matrix-$\boldsymbol{M}_p$ 2-D

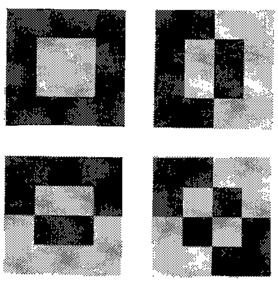

(a) Basis images.

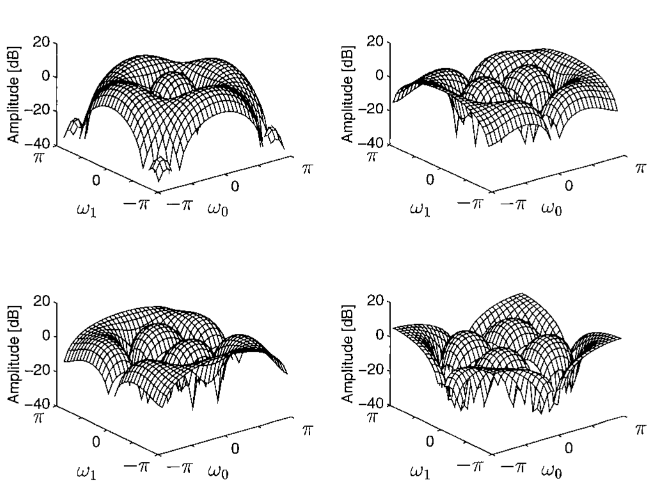

(b) Amplitude responses.

Fig. 5 The type-II lapped Hadamard transform.

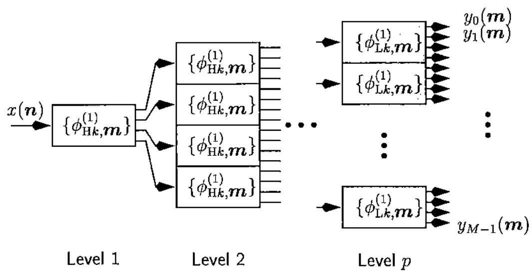

Fig. 6 The tree structure of the $2^p \times 2^p$ LHT.

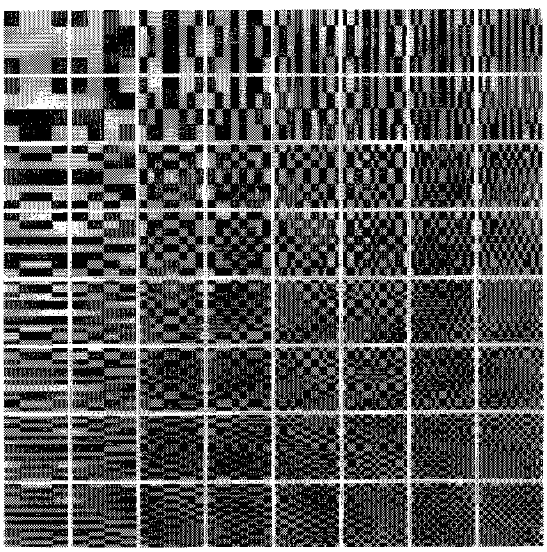

Fig. 7 Basis images of the $2^3 \times 2^3$ type-I LHT.

LHT for $p > 1$ as

$$\boldsymbol{\Phi}_{\mathrm{L}k}^{(p)} = \boldsymbol{\Phi}_{\mathrm{L}((k))_4}^{(1)} \otimes \boldsymbol{\Phi}_{\mathrm{H}\lfloor \frac{k}{4} \rfloor}^{(p-1)}, \tag{33}$$

for $k = 0, 1, \cdots, M-1$. This definition holds all of the orthonormality, AS, BV and overlapping properties.

Equation (33) implies that the matrix-$\boldsymbol{M}_p$ 2-D LHT can be implemented with the tree structure of the matrix-$\boldsymbol{M}_{p-1}$ HT appended with the matrix-$\boldsymbol{M}_1$ LHT as the leaves as shown in Fig. 6, where the hatched box including $\{\phi_{\mathrm{L}k,\boldsymbol{m}}^{(1)}\}$ denotes the matrix-$\boldsymbol{M}_1$ LHT. The inverse transform is simply implemented by reversing the direction of each arrow in the structure.

As an example, we give the basis images of the matrix-$\boldsymbol{M}_3$, that is 8×8-point, type-I LHT in Fig. 7, where each basis image is of size 16×16, while the block size is 8×8. In the same way, we can obtain the basis images of the matrix-$\boldsymbol{M}_p$ LHT.

In the following, we summarize the properties of the 2-D LHT.

- The basis $\{\phi_{\mathrm{L}k,\boldsymbol{m}}^{(p)}\}$ is orthonormal. In addition, the basis images $\phi_{\mathrm{L}k}^{(p)}(\boldsymbol{n})$ are AS, take only BV elements, and have no DC gain for $k \neq 0$, that is, there is no DC leakage [11].
- The basis images $\phi_{\mathrm{L}k}^{(p)}(\boldsymbol{n})$ are *non-separable*, *overlapping*, and of size $2^p \times 2^p$ for the factor $\boldsymbol{M}_p$. The overlapping ratio is 50% for each dimension.

It is important to note again that there is no separable basis which holds the overlapping and AS properties for the matrix-$\boldsymbol{M}_1$ transform. Our proposed LHT, however, achieves those properties by introducing non-separable BV basis.

5. Lattice Structure

In this section, we show a lattice structure of the matrix-$\boldsymbol{M}_1$ LHT, by which the transform can be efficiently implemented.

Figure 8 shows the lattice structure of the matrix-$\boldsymbol{M}_1$ LHT, where γ_n is a parameter of 1 or -1. We give the choices of γ_n for all possible LHTs in Table 1. Types III and IV are other variations, and Types I', II', III' and IV' are sign-reversed versions of the corresponding types, respectively. Note that it is represented as a causal system, although the definition in Eqs. (18), (19), (20) and (21) generate a non-causal one.

In the following, we provide the polyphase representation of the structure for the delay chain $\boldsymbol{d}(\boldsymbol{z}) = (1, z_0^{-1}, z_1^{-1}, z_0^{-1}z_1^{-1})^T$ [9].

$$\boldsymbol{E}(\boldsymbol{z}) = \boldsymbol{\Gamma}_1 \boldsymbol{B} \boldsymbol{\Lambda}(z_1) \boldsymbol{B} \boldsymbol{P}_1 \boldsymbol{B} \boldsymbol{\Lambda}(z_0) \boldsymbol{B} \boldsymbol{P}_0 \boldsymbol{\Gamma}_0 \boldsymbol{E}_0, \tag{34}$$

where

$$\boldsymbol{E}_0 = \frac{1}{2}\begin{pmatrix} 1 & 1 & 1 & 1 \\ 1 & -1 & -1 & 1 \\ 1 & 1 & -1 & -1 \\ 1 & -1 & 1 & -1 \end{pmatrix}, \tag{35}$$

$$\boldsymbol{P}_0 = \begin{pmatrix} 1 & 0 & 0 & 0 \\ 0 & 1 & 0 & 0 \\ 0 & 0 & 0 & 1 \\ 0 & 0 & 1 & 0 \end{pmatrix}, \tag{36}$$

$$\boldsymbol{P}_1 = \begin{pmatrix} 1 & 0 & 0 & 0 \\ 0 & 0 & 1 & 0 \\ 0 & 0 & 0 & 1 \\ 0 & 1 & 0 & \end{pmatrix}, \tag{37}$$

$$\boldsymbol{\Gamma}_0 = \begin{pmatrix} \gamma_0 & 0 & 0 & 0 \\ 0 & \gamma_1 & 0 & 0 \\ 0 & 0 & \gamma_2 & 0 \\ 0 & 0 & 0 & \gamma_3 \end{pmatrix}, \tag{38}$$

$$\boldsymbol{\Gamma}_1 = \begin{pmatrix} -1 & 0 & 0 & 0 \\ 0 & 1 & 0 & 0 \\ 0 & 0 & 1 & 0 \\ 0 & 0 & 0 & -1 \end{pmatrix}, \tag{39}$$

$$\boldsymbol{B} = \frac{1}{\sqrt{2}}\begin{pmatrix} \boldsymbol{I}_2 & \boldsymbol{I}_2 \\ \boldsymbol{I}_2 & -\boldsymbol{I}_2 \end{pmatrix}, \tag{40}$$

$$\boldsymbol{\Lambda}(z) = \begin{pmatrix} \boldsymbol{I}_2 & \boldsymbol{O} \\ \boldsymbol{O} & z^{-1}\boldsymbol{I}_2 \end{pmatrix}. \tag{41}$$

According to Eq. (2), the implementation of the matrix-$\boldsymbol{M}_1$ LHT requires bit shift operation for scaling with 1/4 and 60 additions per block. On the other hand, by using the lattice structure, the implementation complexity is reduced to 24 additions per block with

Table 1 The choices of γ_n parameters for all possible LHTs.

Type	γ_0	γ_1	γ_2	γ_3	Type	γ_0	γ_1	γ_2	γ_3
I	-1	1	1	1	I'	1	-1	-1	-1
II	1	-1	1	1	II'	-1	1	-1	-1
III	-1	-1	1	-1	III'	1	1	-1	1
IV	-1	-1	-1	1	IV'	1	1	1	-1

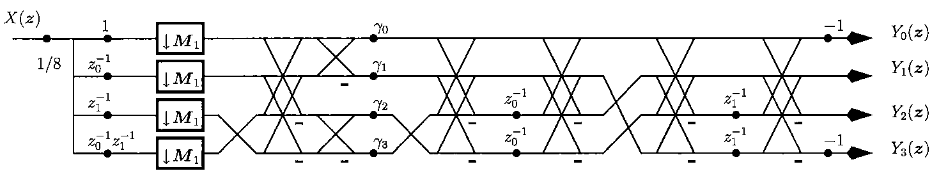

Fig. 8 The lattice structure of the 2×2 LHT.

scaling by 1/8. Obviously, the lattice structure is directly applicable to the tree structure as shown in Fig. 6 so as to efficiently implement it.

The lattice structure can be shown to be minimal (see Appendix B) and that for the inverse transform is simply obtained by choosing $\boldsymbol{R}(\boldsymbol{z}) = \boldsymbol{E}^T(\boldsymbol{z}^{-\boldsymbol{I}})$ from the paraunitary property.

6. Conclusions

In this paper, we proposed a 2-D binary-valued (BV) lapped transform (LT), to which we referred as the lapped Hadamard transform (LHT). LHT has basis images which are axial-symmetric (AS) and take only BV elements ± 1 with a scale of a power of 2. It is known that there is no 2×2-point separable ASLT, By taking non-separable BV basis, our proposed LHT achieves both the AS and overlapping properties for the 2×2-point transform. It was shown that LHT of a larger size is provided with a tree structure, and that LHT can be efficiently implemented by a lattice structure. The characteristic was shown to be very similar to that of the 2-D HT, even if LHT differs from HT in that the basis images are overlapping and non-separable.

References

[1] A.K. Jain, "Fundamentals of Digital Image Processing," Prentice Hall, Englewood Cliffs, 1989.

[2] K.R. Rao and P. Yip, "Discrete Cosine Transform," Academic Press, 1990.

[3] A.M. Tekalp, "Digital Video Processing," Prentice Hall, Inc., 1995.

[4] K. Komatsu and K. Sezaki, "Reversible transform coding of images," IEICE Trans. Fundamentals, vol.J79-A, no.4, pp.981–990, 1996.

[5] T. Mochizuki, "Bit pattern redundancy removal for Hadamard transform coefficients and its application to lossless image coding," IEICE Trans. Fundamentals, vol.J79-A, no.9, pp.1600–1608, 1996.

[6] M.J.T. Smith and T.P. Barnwell III, "Exact reconstruction techniques for tree-structured subband coders," IEEE Trans. Accoust., Speech & Signal Process., vol.34, no.8, pp.434–441, 1986.

[7] H.S. Malvar and D.H. Staelin, "The LOT: Transform coding without blocking effects," IEEE Trans. Accoust., Speech & Signal Process., vol.37, no.4, pp.553–559, 1989.

[8] H.S. Malvar, "Signal Processing with Lapped Transforms," Artech House, 1991.

[9] P.P. Vaidyanathan, "Multirate Systems and Filter Banks," Prentice Hall, Englewood Cliffs, 1993.

[10] M. Vetterli and J. Kovačević, "Wavelets and Subband Coding," Prentice Hall, Englewood Cliffs, 1995.

[11] G. Strang and T.Q. Nguyen, "Wavelets and Filter Banks," Wellesley-Cambridge Press, 1996.

[12] M. Vetterli and D.L. Gall, "Perfect reconstruction FIR filter banks: Some properties and factorizations," IEEE Trans. Accoust., Speech & Signal Process., vol.37, no.7, pp.1057–1071, 1989.

[13] A. K. Soman, P.P. Vaidyanathan, and T.Q. Nguyen, "Linear phase paraunitary filter banks: Theory, factorizations and designs," IEEE Trans. Signal Processing, vol.41, no.12, pp.3480–3496, 1993.

[14] R.L. de Queiroz, T.Q. Nguyen, and K.R. Rao, "Generalized linear-phase lapped orthogonal transforms," Proc. IEEE ISCAS, vol.2, pp.277–280, 1994.

[15] S. Muramatsu and H. Kiya, "A new factorization technique for the generalized linear-phase LOT and its fast implementation," IEICE Trans. Fundamentals, vol.E79-A, no.8, pp.1173–1179, 1996.

[16] S. Muramatsu and H. Kiya, "A new design method of linear-phase paraunitary filter banks with an odd number of channels," Proc. EUSIPCO'96, vol.1, pp.73–76, 1996.

[17] T. Nagai, C.W. Kok, M. Ikehara, and T.Q. Nguyen, "Design and lattice structure of FIR paraunitary filter banks with linear phase," IEICE Trans. Fundamentals, vol.E80-A, no.4, pp.712–721, 1997.

[18] C.W. Kok, T. Nagai, M. Ikehara, and T.Q. Nguyen, "Structures and factorizations of linear phase paraunitary filter banks," Proc. IEEE ISCAS, pp.365–368, 1997.

[19] J. Kovačević and M. Vetterli, "Nonseparable two and three-dimensional wavelets," IEEE Trans. Signal Processing, vol.43, no.5, pp.1269–1273, 1995.

[20] S. Muramatsu, A. Yamada, and H. Kiya, "A design method of multidimensional linear-phase paraunitary filter banks with a lattcie structure," IEICE Technical Report, DSP97-40, 1997.

[21] S. Muramatsu, A. Yamada, and H. Kiya, "A design method of multidimensional linear-phase paraunitary filter banks with a lattcie structure," Proc. IEEE TENCON'97, vol.1, pp.69–72, 1997.

[22] M.J.T. Smith and S.L. Eddins, "Analysis/synthesis techniques for subband image coding," IEEE Trans. Accoust., Speech & Signal Process., vol.38, no.8, pp.1446–1456, 1990.

[23] H. Kiya, K. Nishikawa, and M. Iwahashi, "A development of symmetric extension method for subband image coding," IEEE Trans. Image Processing, vol.3, no.1, pp.78–81, 1994.

[24] R.H. Bamberger, S.L. Eddins, and V. Nuri, "Generalized symmetric extension for size-limited multirate filter banks," IEEE Trans. Image Processing, vol.3, no.1, pp.82–87, 1994.

[25] L. Chen, T.Q. Nguyen, and K.-P. Chan, "Symmetric extension methods for M-channel PR LP FIR analysis/synthesis systems," Proc. IEEE ISCAS, vol.2, pp.277–280, 1994.

Appendix A: Choices of $\boldsymbol{\Theta}$

In the following, we show all possible choices of the matrix $\boldsymbol{\Theta}$ which satisfies Eq. (17).

Let θ_{ij} be the i, j-th element of the matrix $\boldsymbol{\Theta}$. Then, from Eq. (17), θ_{ij} must satisfy the following equations:

$$\theta_{00}^2 + \theta_{01}^2 + \theta_{10}^2 + \theta_{01}^2 = \frac{1}{4} \qquad \text{(A}\cdot\text{1)}$$

$$\theta_{00}\theta_{01} + \theta_{10}\theta_{11} = 0 \qquad \text{(A}\cdot\text{2)}$$

$$\theta_{00}\theta_{10} + \theta_{01}\theta_{11} = 0 \qquad \text{(A}\cdot\text{3)}$$

$$\theta_{00}\theta_{11} + \theta_{01}\theta_{10} = 0 \qquad \text{(A}\cdot\text{4)}$$

Suppose that each element θ_{ij} is non-zero. In this case, Eqs. (A·2), (A·3) and (A·4) lead the following equation:

$$\theta_{00} = -\frac{\theta_{10}\theta_{11}}{\theta_{01}} = -\frac{\theta_{01}\theta_{11}}{\theta_{10}} = -\frac{\theta_{01}\theta_{10}}{\theta_{11}}. \qquad \text{(A}\cdot\text{5)}$$

The above equation implies that $\theta_{10}^2\theta_{11}^2 = \theta_{01}^2\theta_{11}^2 =$

$\theta_{01}^2\theta_{10}^2$, that is, $\theta_{01}^2 = \theta_{10}^2 = \theta_{11}^2$. By expressing another element as in Eq. (A· 5), we have the relation

$$\theta_{00}^2 = \theta_{01}^2 = \theta_{10}^2 = \theta_{11}^2. \qquad \text{(A· 6)}$$

Namely, if $\boldsymbol{\Theta}$ consists of non-zero elements, then the absolute value of each elements must be the same as each other. In other words, $\boldsymbol{\Theta}$ must be BV. From Eq. (A· 1), the absolute value results in $\frac{1}{4}$.

Next, let us consider the number of negative elements in $\boldsymbol{\Theta}$. Clearly, Eqs. (A· 2), (A· 3) and (A· 4) are satisfied, if and only if one term is positive and the other is negative. It is obvious that the condition is achieved if and only if the number of negative elements is one or three.

If $\boldsymbol{\Theta}$ has zero-value elements, then the number of them must be three, otherwise it conflicts Eqs. (A· 2), (A· 3) and (A· 4).

Appendix B: Minimality of Lattice Structure

A structure is said to be *minimal* if it uses the minimum number of delay elements for its implementation [9]. For a 1-D causal PU system $\boldsymbol{E}(z)$, it is known that $\deg(\det(\boldsymbol{E}(z))) = \deg(\boldsymbol{E}(z))$, where $\deg(\boldsymbol{H}(z))$ denotes the degree of $\boldsymbol{H}(z)$, that is, the minimum number of delay elements required to implement $\boldsymbol{H}(z)$.

Now, let us investigate the degree of our proposed structure. Note that the degree in terms of the 0-th (or 1-th) dimension delay element z_0^{-1} (or z_1^{-1}) can not be increased by choosing any value of delay elements of the other dimension. Therefore, the following inequality holds.

$$\deg^{\{d\}}(\boldsymbol{E}(\boldsymbol{z})) \geq \deg^{\{d\}}\left(\boldsymbol{E}(\boldsymbol{z}^{\{d\}})\right), \quad d = 0, 1, \qquad \text{(A· 7)}$$

where $\deg^{\{d\}}(\boldsymbol{E}(\boldsymbol{z}))$ denotes the degree in terms of z_d^{-1}, $\boldsymbol{z}^{\{0\}} = (z_0\ 1)^T$ and $\boldsymbol{z}^{\{1\}} = (1\ z_1)^T$.

From, Eq. (34), it can be verified that our proposed structure has

$$\deg^{\{d\}}\left(\det\left(\boldsymbol{E}(\boldsymbol{z}^{\{d\}})\right)\right) = 2, \quad d = 0, 1. \qquad \text{(A· 8)}$$

This equation implies that $\deg^{\{d\}}(\boldsymbol{E}(\boldsymbol{z}^{\{d\}})) = 2$ for $d = 0, 1$, since $\boldsymbol{E}(\boldsymbol{z}^{\{d\}})$ can be regarded as a 1-D causal PU system $\boldsymbol{E}(z_d)$. Consequently, we have

$$\deg^{\{d\}}(\boldsymbol{E}(\boldsymbol{z})) \geq 2, \quad d = 0, 1. \qquad \text{(A· 9)}$$

The last inequality guarantees that our structure is minimal, since it implements the LHT with only two delay elements for each dimension.

Shogo Muramatsu was born in Tokyo, Japan, on May 2, 1970. He received the B.E. and M.E. degrees in electrical engineering from Tokyo Metropolitan University, Tokyo, Japan in 1993 and 1995, respectively. In 1997, he joined Tokyo Metropolitan University, where he is curently a research associate of Electrical Engineering, Graduate School of Engineering. His research interests are in digital signal processing, multirate systems, and image processing. Mr. Muramatsu is a Member of the Institute of Electrical and Electronics Engineers, Inc. (IEEE) of USA.

Akihiko Yamada was born in Osaka, Japan, on September 5, 1936. He received the B.E. and the D.E. degrees from Osaka University, Osaka, Japan in 1955 and 1980, respectively. In 1955, he joined NEC Corporation. In 1993, he joined Tokyo Metropolitan University, where he is currently a Professor of Electrical Engineering, Graduate School of Engineering. His research interests are in hardware/software codesign and VLSI design methodologies. Dr. Yamada is a senior member of the Institute Electrical and Electronics Engineers, Inc. (IEEE) of USA, and a member of the Association for Computing Machinery (ACM) of USA and Information Processing Society of Japan.

Hitoshi Kiya was born in Yamagata, Japan, on November 16, 1957. He received the B.E. and M.E. degrees in electrical engineering from Nagaoka University of Technology, Niigata, Japan, and the D.E. degree in electrical engineering from Tokyo Metropolitan University, Tokyo, Japan, in 1980, 1982 and 1987, respectively. In 1982, he joined Tokyo Metropolitan University, where he is currently an Associate Professor of Electrical Engineering, Graduate School of Engineering. He was a visiting researcher of the University of Sydney in Australia from Oct.1995 to Mar.1996. His research interests are in digital signal processing, multirate systems, adaptive filtering, image processing, and efficient algorithms for VLSI implementation. Dr. Kiya is a Member of the Institute Electrical and Electronics Engineers, Inc. (IEEE) of USA, the Image Electronics Engineers of Japan and the Institute of Image Information and Television Engineers of Japan. He is an Associate Editor of IEEE Transactions on Signal Processing.